Biosensors and Bioelectronics 222 (2023) 115002

Contents lists available at ScienceDirect

Biosensors and Bioelectronics

journal homepage: www.elsevier.com/locate/bios

FELICX: A robust nucleic acid detection method using flap endonuclease and CRISPR-Cas12

Nikhil Aggarwal [a,b], Yuanmei Liang [a,b,c], Jee Loon Foo [a,b,c], Hua Ling [a,b,c], In Young Hwang [a,b,c], Matthew Wook Chang [a,b,c,*]

[a] NUS Synthetic Biology for Clinical and Technological Innovation (SynCTI), National University of Singapore, Singapore
[b] Synthetic Biology Translational Research Programme, Yong Loo Lin School of Medicine, National University of Singapore, Singapore
[c] Department of Biochemistry, Yong Loo Lin School of Medicine, National University of Singapore, Singapore

ARTICLE INFO

Keywords:
CRISPR
Nucleic acid detection
Endonuclease
Single-nucleotide polymorphisms
Diagnostics

ABSTRACT

Nucleic acid detection is crucial for monitoring diseases for which rapid, sensitive, and easy-to-deploy diagnostic tools are needed. CRISPR-based technologies can potentially fulfill this need for nucleic acid detection. However, their widespread use has been restricted by the requirement of a protospacer adjacent motif in the target and extensive guide RNA optimization. In this study, we developed FELICX, a technique that can overcome these limitations and provide a useful alternative to existing technologies. FELICX comprises flap endonuclease, Taq ligase and CRISPR-Cas for diagnostics (X) and can be used for detecting nucleic acids and single-nucleotide polymorphisms. This method can be deployed as a point-of-care test, as only two temperatures are needed without thermocycling for its functionality, with the result generated on lateral flow strips. As a proof-of-concept, we showed that up to 0.6 copies/μL of DNA and RNA could be detected by FELICX in 60 min and 90 min, respectively, using simulated samples. Additionally, FELICX could be used to probe any base pair, unlike other CRISPR-based technologies. Finally, we demonstrated the versatility of FELICX by employing it for virus detection in infected human cells, the identification of antibiotic-resistant bacteria, and cancer diagnostics using simulated samples. Based on its unique advantages, we envision the use of FELICX as a next-generation CRISPR-based technology in nucleic acid diagnostics.

1. Introduction

Nucleic acids such as DNA and RNA are important biomarkers, with their detection enabling the diagnosis of a wide range of acute and chronic diseases—particularly infections and, more recently, cancer (Bronkhorst et al., 2019). Therefore, accurate, rapid, and cost-effective methods for nucleic acid detection can play a vital role in disease control and management. This was exemplified during the coronavirus disease 2019 (COVID-19) pandemic, wherein detecting the SARS-CoV-2 viral genome was critical for identifying COVID-19-positive cases and shaping control measures to reduce widespread viral transmission (Drain, 2022).

There are many methods of nucleic acid detection currently available, with varying specificity, sensitivity, simplicity, and speed. Among these methods, PCR-based technologies are the gold standard for nucleic acid diagnostics (Gootenberg et al., 2017; Kaminski et al., 2021). However, the need for sophisticated equipment, expensive reagents, and trained personnel hinders their use as point-of-care diagnostic tests (Yang and Rothman, 2004). To address these limitations, clustered regularly interspaced short palindromic repeat (CRISPR)-Cas systems have been repurposed to develop rapid (less than 1 h), highly sensitive (subattomolar range), and programmable nucleic acid-based diagnostic tests requiring minimal equipment (reviewed in Kaminski et al., 2021). Many of these tests utilize the *trans* cleavage activity of Cas12 or Cas13, wherein a fluorescent reporter DNA or RNA is cleaved off in the presence of the target DNA or RNA, respectively (Chen et al., 2018; Kellner et al., 2019). CRISPR-based diagnostic tests have since been used to detect the SARS-CoV-2 (Broughton et al., 2020), Zika, and dengue viruses (Gootenberg et al., 2017), as well as *Mycobacterium tuberculosis* (Ai et al., 2019), *Plasmodium falciparum* (Cunningham et al., 2021), Epstein–Barr virus (EBV) (Wu et al., 2019), and *Salmonella enterica* (Shen et al., 2020).

Despite the advantages of CRISPR-based diagnostics, there are key limitations that restrict its widespread use. For instance, the Cas protein's ability to successfully detect nucleic acids requires the presence of

* Corresponding author. NUS Synthetic Biology for Clinical and Technological Innovation (SynCTI), National University of Singapore, Singapore.
E-mail address: bchcmw@nus.edu.sg (M.W. Chang).

https://doi.org/10.1016/j.bios.2022.115002
Received 11 October 2022; Received in revised form 26 November 2022; Accepted 7 December 2022
Available online 9 December 2022
0956-5663/© 2022 The Authors. Published by Elsevier B.V. This is an open access article under the CC BY license (http://creativecommons.org/licenses/by/4.0/).

a protospacer adjacent motif (PAM) flanking the target sequence—e.g., TTTN for Cas12a. This can prevent the detection of single-nucleotide polymorphisms (SNPs) not flanked by a PAM and shorter targets without the PAM sequence (Li et al., 2019). The off-target binding and mismatch tolerance of the single guide RNA (sgRNA) may also cause false signals, leading to misinterpretation(Vangah et al., 2020), thus requiring the use of software packages for sgRNA design (Kaminski et al., 2021).

In this study, we developed FELICX, comprising flap endonuclease, Taq ligase and CRISPR-Cas for diagnostics (X). This system can detect any region of DNA or RNA with single-base pair resolution without being constrained by the presence of a PAM in the target and sgRNA activity. FELICX is a novel nucleic acid detection method that can overcome the limitations of existing CRISPR-based technologies by using a flap endonuclease (FEN) instead of CRISPR-Cas12 to probe the amplified target. To develop FELICX, we first characterized a FEN mutant and optimized its cleavage activity. Second, we incorporated the FEN and Taq ligase into a one-pot reaction to form the substrate for CRISPR-Cas12 and showed the functionality of FELICX using purified SARS-CoV-2 nucleic acids as the target. Third, we improved the sensitivity and usability of FELICX by including isothermal amplification and detecting the final result on lateral flow strips. Finally, we demonstrated the versatility of FELICX by reprogramming it to detect a SARS-CoV-2 variant in simulated samples, EBV in human cells, an antibiotic resistance gene in pathogenic *Klebsiella pneumoniae*, and a cancer biomarker in serum with high specificity and sensitivity.

2. Results

2.1. Working principle and advantages of nucleic acid detection by FELICX

Nucleic acid detection using FELICX involves sample lysis to release genetic material followed by target amplification using an isothermal amplification technique (Fig. 1a). The amplified product is then detected using FELICX, with the output signal measured by a fluorescence reader or lateral flow strips (Fig. 1b and c). FELICX comprises three enzymes, namely: FEN, Taq ligase, and Cas12—all working in tandem to detect DNA or RNA. First, a pair of oligos, known as the invading and flap primers, bind to the target DNA/RNA such that the flap primer creates a noncomplementary 5′-flap (Fig. 1b). This flap structure is recognized by FEN in a sequence-independent manner and is then cleaved off. The flap primer is designed such that its melting temperature is similar to the temperature at which cleavage occurs. This causes cyclic annealing and denaturing of the flap primer, resulting in multiple cleaved flaps being generated from a single target. Second, the cleaved flap is ligated to a unique double-stranded DNA adaptor by Taq ligase. This creates the target sequence recognized by the Cas12-sgRNA complex in the final step. Upon target recognition, Cas12 cleaves a DNA reporter via its *trans* activity, which results in either the production of a fluorescence signal or the disappearance of a specific band on the lateral flow strip.

The main difference between FELICX and other CRISPR-based technologies is that the amplified product is recognized by FEN instead of Cas12. This is advantageous, as the activity of FEN is independent of the target sequence, unlike Cas12, which requires the PAM to be adjacent to the target (Fig. 1d). Essentially, any region in the nucleic acid can be probed by FEN as long as the invading and flap primers bind

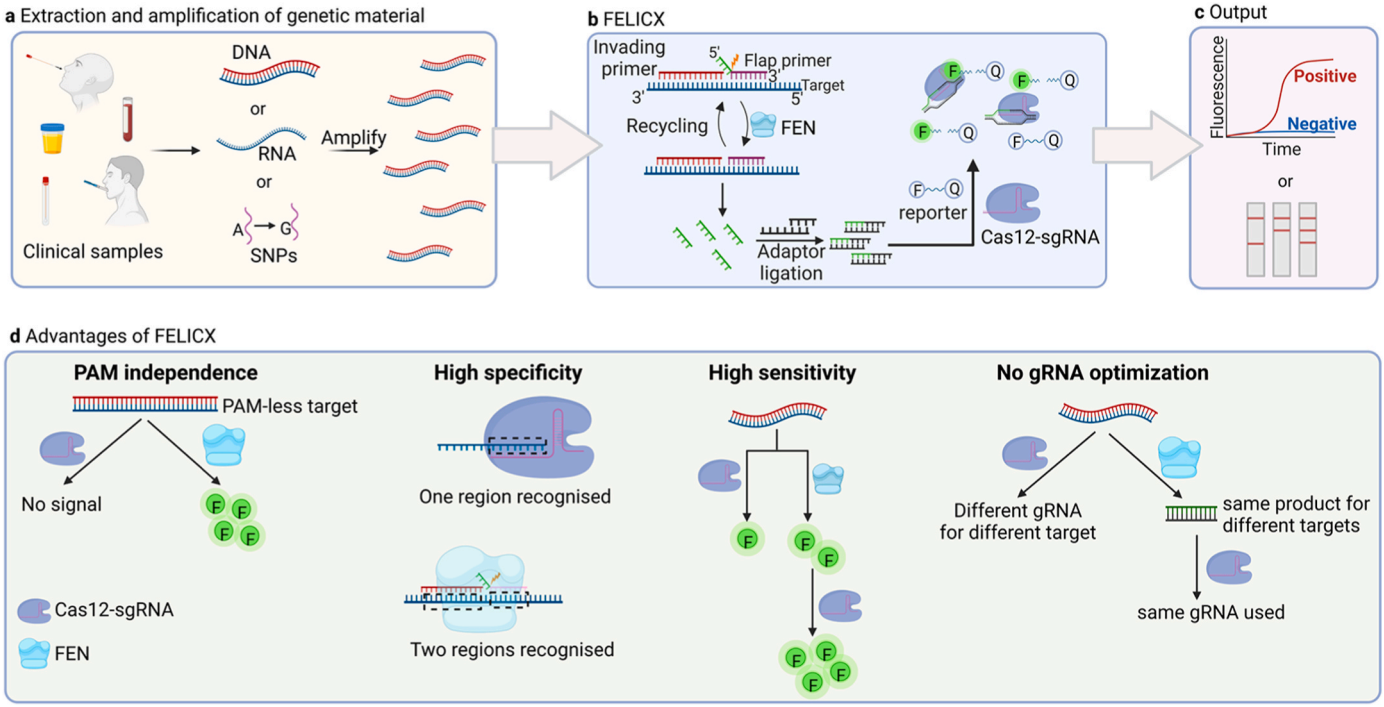


Fig. 1. Illustration of the workflow and advantages of FELICX for nucleic acid detection. (a)-(c) Outline of nucleic acid detection from clinical samples to the final output using isothermal amplification and FELICX. In the first step, (a) genetic material is extracted from clinical samples and amplified isothermally. This amplified product is subjected to (b) FELICX comprising FEN activity, adaptor ligation, and the Cas12-sgRNA reactions occurring sequentially. The output of FEN activity on the target is an oligo (green) that is ligated to an adaptor to form the substrate for Cas12-sgRNA, which cleaves a ssDNA reporter. (c) The output can be either a fluorescence signal or a readout on lateral flow strips. (d) Advantages of FELICX compared to other CRISPR-Cas12 techniques for nucleic acid diagnostics. These include 1) PAM independence, as the nucleic acid target is probed by FEN in a sequence-independent manner; 2) high specificity, as two regions are recognized by FEN compared to only one by Cas12; 3) high sensitivity, as both FEN and Cas12 amplify the signal compared to only Cas12 signal amplification in current methods; and 4) no requirement for gRNA optimization, as the same product is formed after FEN and adaptor ligation irrespective of the target sequence enabling detection using the same gRNA.

to the target and create a 5′-flap structure. As a pair of oligos must bind to the target, detection by FEN has a higher specificity than that by Cas12, which requires only the region complementary to its sgRNA for activity (Fig. 1d). In addition, FELICX comprises two signal amplification components: FEN and CRISPR-Cas12, resulting in a higher sensitivity compared to that of CRISPR-based technologies where CRISPR-Cas12 is the sole signal amplifier (Fig. 1d). Finally, since FEN activity is sequence-independent, the same dsDNA product is formed after the FEN and Taq ligase reaction for every target (Fig. 1d). This product can then be detected by the Cas12-sgRNA complex without changing the gRNA sequence. Thus, new targets can be detected without optimizing the gRNA activity, unlike current CRISPR-based technologies that require gRNA optimization for the detection of every new target (Fig. 1d).

2.2. Characterization and optimization of FEN

To develop FELICX, we first characterized and optimized the cleavage activity of FEN. FENs are a class of enzymes ubiquitous in both prokaryotes and eukaryotes. The main role of FEN is in DNA replication, where it removes the RNA primer from the 5′-end of the Okazaki fragments that are subsequently joined together to form the lagging strand (Balakrishnan and Bambara, 2013). In bacteria, DNA polymerase I—which consists of an N-terminal 5′ nuclease and a C-terminal polymerase—plays the role of FEN via its N-terminal domain (Xu et al., 1997). In archaea and mammalian cells, there is a dedicated FEN enzyme similar to the N-terminal domain of bacterial DNA polymerase I (Balakrishnan and Bambara, 2013).

FEN has been used to detect both DNA (Lyamichev et al., 1999b) and RNA (Eis et al., 2001), although it has several limitations, such as its slow speed, need for initial denaturation to assemble the oligos on the target, and reliance on a fluorescence reader for signal detection. DNA polymerase I from *Thermus thermophilus* (Tth pol) is a well-characterized FEN that can recognize the flap structure on both DNA and RNA targets (Eis et al., 2001). To determine if Tth pol is the best candidate for FELICX, we expressed and purified a panel of Tth pol variants, the N-terminal domain of Tth pol (TthN), human FEN1 (hFEN), archaeal *Methanococcus jannaschii* FEN1 (MjaFEN), bacteriophage T5

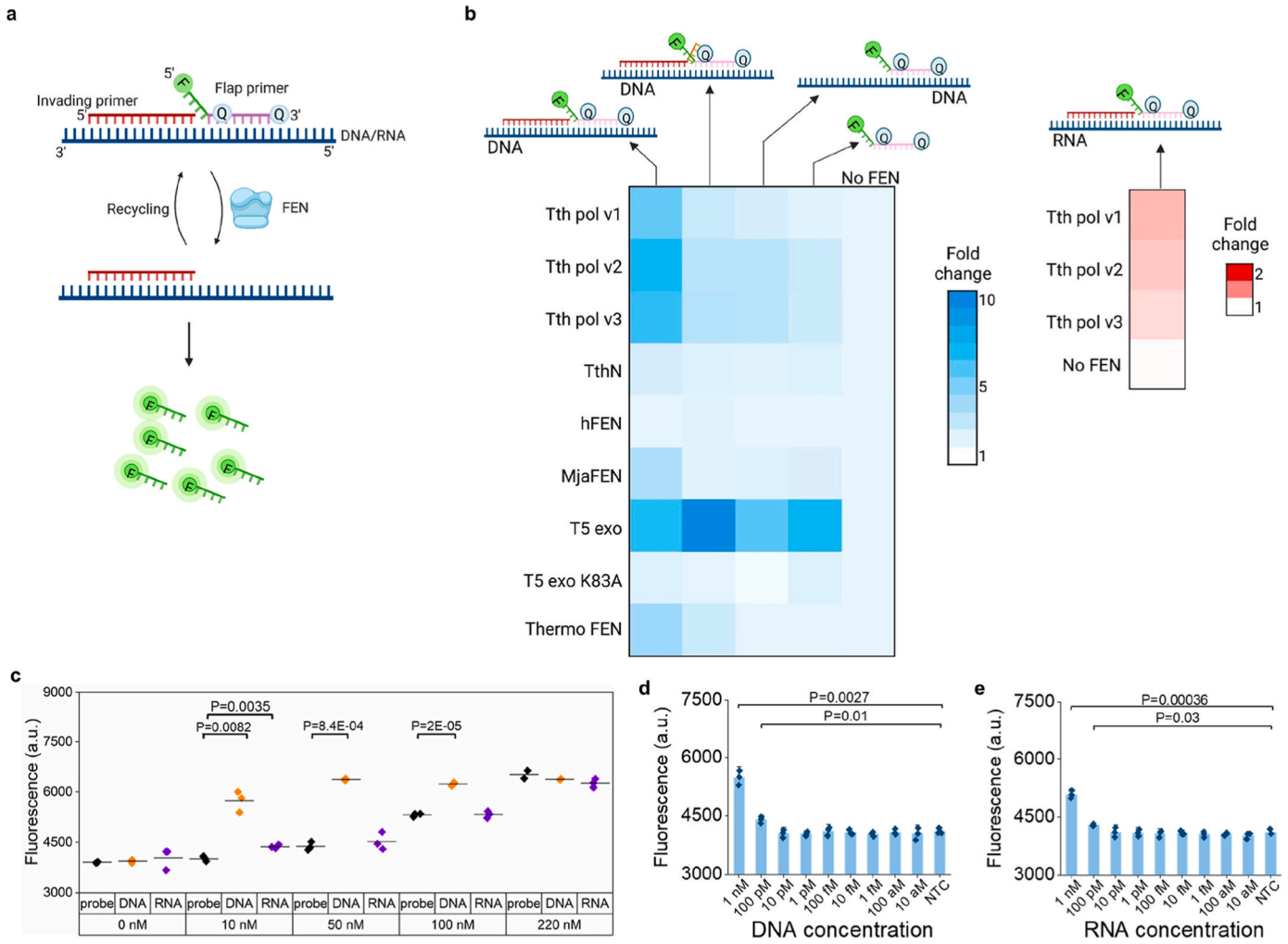


Fig. 2. Comparison of FEN activity of different enzymes and its optimization. (a) Schematic of the fluorescence assay for quantifying FEN activity. (b) The activity of different FEN enzymes on 1 nM *orf1ab* DNA/RNA substrate with different configurations of the flap and invading primers, including the configuration shown in (a), a double flap configuration with flaps on both invading and flap primers as shown in Fig. S1d, a configuration without the invading primer, and a configuration with the flap primer only. No FEN refers to the reaction without the enzyme. The data (blue for DNA substrate and red for RNA substrate) represent the mean (n = 3 biological repeats). Thermo FEN was obtained from NEB (Catalog No. M0645S). (c) FEN activity of Tth pol v2 on the probe (flap primer only), DNA (1 nM) and RNA (1 nM) substrates at different enzyme concentrations after 60 min of incubation at 65 °C. The horizontal black bars represent the mean (n = 3 biological repeats). The p value < 0.05 are provided, calculated using a two-sample *t*-test. (d) and (e) Detection limits of *orf1ab* DNA and RNA, respectively, after incubation with 10 nM Tth pol v2 for 30 min at 65 °C. The data represents the mean ± SD (n = 3 biological repeats). The p value < 0.05 compared to NTC are provided, calculated using a two-sample *t*-test. NTC - no target control.

exonuclease (T5 exo) (Figs. S1a and c) and compared their activities with a commercially available thermostable FEN (thermo FEN) (Fig. 2b). Previously, wild-type Tth pol was mutated (G506K, Q509K, H786A) to enable RNA recognition and inactivate the polymerase domain (Eis et al., 2001). This mutant is named Tth pol v1 in this study. Mutations in Taq polymerase have also been reported to expand its substrate spectrum, although their effect on the FEN activity of the enzyme was not studied (Ong et al., 2006; Xia et al., 2002). These mutations lie in the polymerase domain of the enzyme and may affect its substrate binding and, consequently, FEN activity. Due to the high similarity between the Taq and Tth polymerases, we hypothesized that corresponding mutations in Tth pol might have a similar effect on the enzyme activity. Therefore, we further mutated Tth pol v1 to include the A604V, A610V, I616M, and E617GA mutations, creating Tth pol v2. Similarly, Tth pol v1 was mutated to include the A599T, W606R, A607Q, and I616T mutations to create Tth pol v3 (Fig. S1b). We also created TthN, comprised only of the N-terminal domain (amino acids 1–307) of full-length Tth pol, and tested its FEN activity based on a previous report showing that the N-terminal domain of Taq polymerase alone exhibits FEN activity (Lyamichev et al., 1999a).

To quantify FEN activity, we used a flap primer with a 5′ fluorophore and two attached quenchers—3′ and internal—which would generate a fluorescence signal upon cleavage by FEN (Fig. 2a). For all the FEN enzymes, we tested the enzyme activity on different configurations of the flap and invading primers: the 5′-flap of the flap primer and an invading primer (Fig. 2a), the double flap wherein both the flap and invading primers have flaps (Fig. S1d), as well as in the absence of the target-specific invading primer. We also measured the nonspecific activity of FEN on the fluorophore-quencher flap primer alone. For the target, we used a partial *orf1ab* DNA of SARS-CoV-2 with low similarity to the SARS viral genome (Fig. S2). The reaction was performed at 65 °C, which is the melting temperature of the flap primer used in this study.

As seen in the left panel of Fig. 2b, the activity of Tth pol v1, v2, and v3 was greatly reduced when the double flap substrate was used (Fig. S1d) and when the invading primer was missing, suggesting that the configuration shown in Fig. 2a is the best for these enzymes. Among these variants of Tth pol, Tth pol v2 showed the highest activity, followed by Tth pol v3 and v1 (Fig. 2b), on the DNA substrate to which the flap primer and an invading primer without the flap were bound, validating our hypothesis that mutations introduced in the enzyme affect the enzyme activity. Fluorescence signals were also observed in the case of the flap primer alone (Fig. 2b), indicating that the enzymes had low nonspecific activity along with high specific FEN activity. Surprisingly, TthN did not show any activity for any of the substrates tested, contrary to a previous study performed using the highly similar N-terminal domain of Taq polymerase(Lyamichev et al., 1999a). hFEN did not show any activity, likely due to the high reaction temperature, while the thermophilic MjaFEN displayed poor activity for the substrate with the 5′-flap of the flap primer and an invading primer (Fig. 2b). For T5 exo, strong fluorescence signals were observed for all substrates, including the flap primer alone, almost immediately after initiating the reaction. This indicates that the enzyme has very high exonuclease activity that masks its FEN activity. To abolish its exonuclease activity, we mutated the K83 residue, which has been shown to be essential for exonuclease but not endonuclease activity (Garforth et al., 1999). However, in our study, the K83A mutation completely inactivated the enzyme, abolishing both endo- and exonuclease activities (Fig. 2b). Meanwhile, thermo FEN showed a similar trend of activity with the various DNA substrates as Tth pol. However, compared to Tth pol and its variants, it had lower activity. These results indicate that Tth pol v2 is the best candidate with high specific FEN activity and that the ideal substrate for the enzyme is the DNA target bound to a flap primer and an invading primer without a flap.

Next, we selected the best FEN candidate, Tth pol v2, and compared its activity with the other Tth pol variants, v1 and v3, on an RNA substrate to which the flap primer and the invading primer with the flap were bound. Similar to the previous experiment, we used the partial *orf1ab* RNA of SARS-CoV-2 for the assay. As seen in the right panel of Fig. 2b, Tth pol v1 and v2 performed better than Tth pol v3, although weaker signals were observed for all three enzymes compared to the DNA substrate. Based on the FEN activity observed on both DNA and RNA substrates, we selected Tth pol v2 as the FEN for FELICX. Further mutagenesis of Tth pol v2 did not significantly improve the FEN activity of the enzyme (Supplementary result: Mutagenesis of Tth pol v2).

We further characterized Tth pol v2 by evaluating the effect of enzyme concentration on FEN activity on both DNA and RNA substrates and the nonspecific activity on the flap primer alone (labeled as probe). We observed that with increasing enzyme concentrations, there was a concomitant increase in nonspecific activity, as indicated by the increasing fluorescence with the probe alone (Fig. 2c). At 10 nM, nonspecific activity was minimal, with high FEN activity observed for both DNA and RNA substrates. Beyond this concentration, nonspecific activity significantly increased, subsequently becoming indistinguishable from FEN activity at 220 nM. This suggests that an optimal concentration (10 nM) of the enzyme is needed for specific FEN activity.

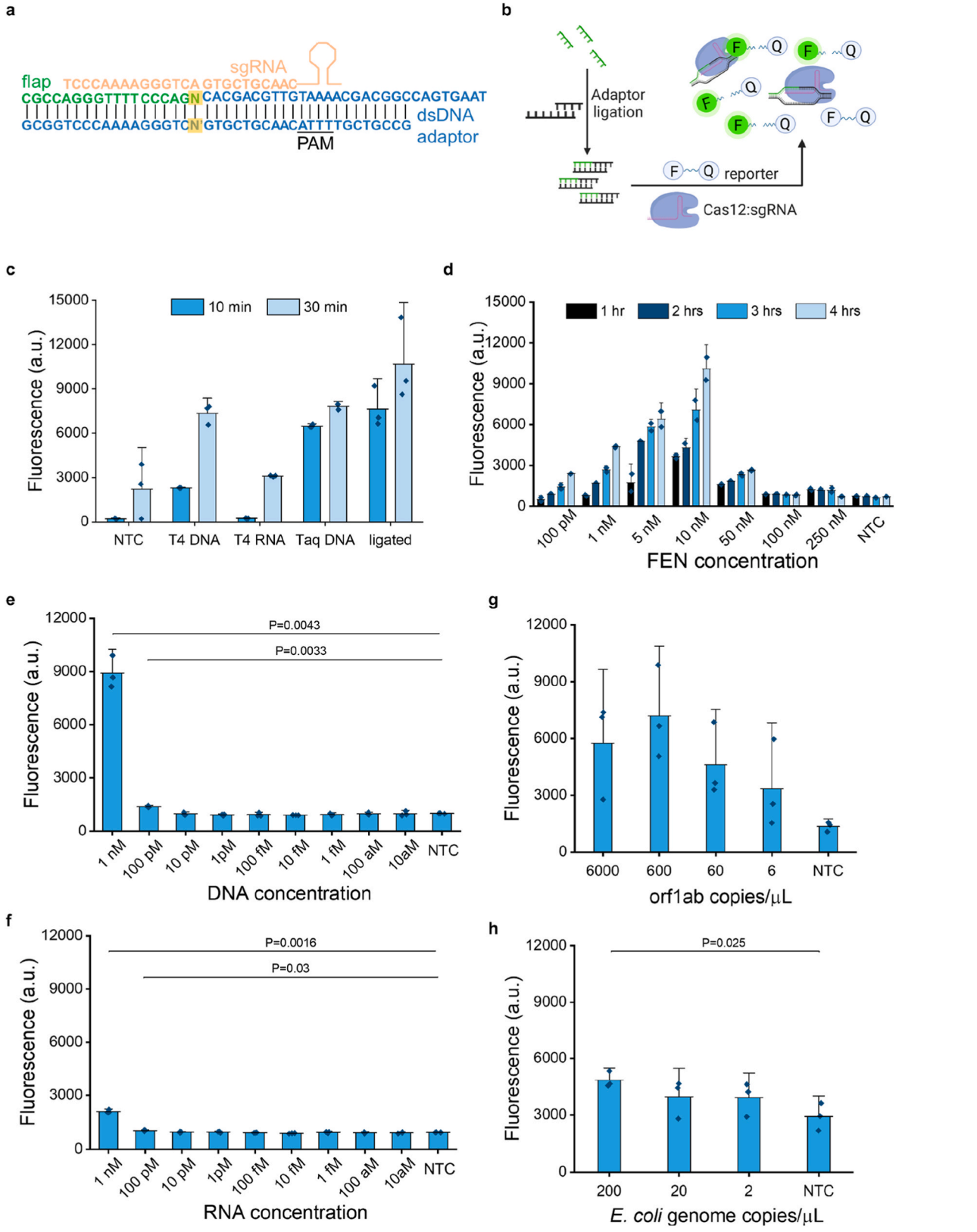
Although FEN can amplify signals through the cyclic annealing and denaturing of the flap primer, we hypothesized that it is unlikely to be robust enough for the highly sensitive detection of the target in a short time due to the linear amplification of the signal (one flap product formed every cycle per target). To confirm this, we ascertained the detection limit for both DNA and RNA by using 10 nM Tth pol v2. Within 30 min of incubation, we only detected up to 100 pM of both DNA and RNA, although the fluorescence signal for 100 pM was slightly higher than that for the no target control (NTC) (Fig. 2d and e). Increasing the Tth pol v2 concentration to 50 nM worsened the detection limit to 1 nM, as expected, due to higher nonspecific activity resulting in greater background fluorescence (Fig. S4). This demonstrates the need for further signal amplification to enable highly sensitive target detection by FEN.

2.3. Development and optimization of FELICX

CRISPR-Cas12 acts as an excellent signal amplifier through its rapid *trans* cleavage activity on ssDNA upon recognition of the DNA substrate (Qiu et al., 2022). Thus, we combined FEN with CRISPR-Cas12 by converting the flap oligo generated by FEN to the substrate for Cas12 through ligation to an adaptor. For FELICX, we used Cas12 from *Lachnospiraceae bacterium* ND2006, which has previously been used for nucleic acid detection (Broughton et al., 2020). As Cas12 has a preference for a dsDNA substrate over ssDNA (Fig. S5), we created a dsDNA adaptor with a 3′ overhang by annealing two oligos: 5′p-adaptor and ds-convertor. The 5′p-adaptor has a 5′-phosphate that is ligated to the 3′-OH of the flap oligo by a ligase enzyme, while the ds-convertor carries the PAM adjacent to the binding site of sgRNA (Fig. 3a). The complementary target of the sgRNA is split between the flap and the adaptor, which ensures that neither the adaptor alone nor the uncleaved flap primer produces a signal.

For every new target in FELICX, only the invading primer and the part of the flap primer complementary to the target must be changed (Fig. 2a). The 5′ flap of the flap primer remains constant, as FEN can cleave the flap primer in a sequence-independent manner. However, the cleavage site for FEN is one base pair into the complementary part of the flap primer with the target. Thus, every target can produce a flap with either of the four nucleotides at the 3′ end of the flap, depending on the target sequence. To account for this, the complementary nucleotide in the ds convertor must be changed (see nucleotides N and N′ in Fig. 3a). As this base pair falls within the region recognized by the sgRNA, we tested whether the Cas12-sgRNA complex could recognize the dsDNA adaptor with either of the four nucleotides at position N without changing the sgRNA sequence. This would simplify the use of Cas12-sgRNA, eliminating the need for changes in the sgRNA sequence for every new target. For this, we used the Cas12-sgRNA complex with the

sgRNA complementary to the dsDNA adaptor with thymine at position N (Fig. S6a). As shown in Fig. S6c, Cas12-sgRNA detected all possible targets with similar efficiency, irrespective of the nucleotide at the end of the flap. This is expected, as previous reports have shown that LbCas12a can tolerate mismatches in nucleotides 8–18 from the PAM (Li et al., 2018), which is the region where the fickle base pair (N–N′) lies. Therefore, for any nucleic acid target, the remaining part of the dsDNA adaptor apart from one base pair and the sgRNA remain unchanged, irrespective of the target sequence, enabling easier reprogramming of FELICX to detect different targets.



(caption on next page)

Fig. 3. Optimization of the adaptor ligation and nucleic acid detection limits using FELICX. (a) Sequence of the flap product (green) ligated to the dsDNA adaptor (blue). The sgRNA bound to the adaptor is also shown in orange. The PAM is underlined and the fickle base pair is shaded in yellow. (b) Ligation of an oligo, similar to the flap product formed by FEN, to the dsDNA adaptor by a ligase. The ligated product forms the substrate for Cas12-sgRNA, which, upon activation, cleaves a ssDNA reporter, resulting in the production of a fluorescence signal. (c) Fluorescence signal observed after ligating the synthetic flap oligo with the dsDNA adaptor for 30 min using different ligases and subsequent detection by Cas12-sgRNA (10 min or 30 min of cleavage). The ligation volume was 15 μL, to which 5 μL of Cas12-sgRNA was subsequently added. The data represents the mean ± SD (n = 3 biological repeats). NTC - no target control. Ligated - preligated substrate. (d) Optimization of the FEN concentration and incubation time for the FEN + Taq ligase reaction (15 μL) using *orf1ab* DNA (1 nM). After ligation, the Cas12-sgRNA reaction (20 μL) was performed for 30 min. The data represents the mean ± SD (n = 2 biological repeats). NTC- no target control. (e) and (f) Detection limit of *orf1ab* DNA or RNA spiked into purified HEK293T total DNA or RNA, respectively, using FELICX. The FEN + Taq ligase reaction (20 μL) was performed for 4 h and the Cas12-sgRNA reaction (an additional 7 μL) was performed for 30 min. The data represents the mean ± SD (n = 3 biological repeats). The p value < 0.05 compared to NTC are provided, calculated using a two-sample *t*-test. NTC - no target control. (g) and (h) Detection limit of HDA + FELICX for the *orf1ab* DNA and *E. coli* genome spiked into HEK293T total DNA. HDA was performed for 1 h in a 10 μL reaction, FEN + Taq ligase reaction for 1 h (total volume 20 μL), and Cas12-sgRNA reaction for 30 min (total volume 27 μL). The data represents the mean ± SD (n = 3 biological repeats). The p value < 0.05 compared to NTC are provided, calculated using a two-sample *t*-test. NTC - no target control.

For the ligation of the flap to the adaptor, Taq ligase is the ideal option, as its optimal temperature (65 °C) is the same as that of FEN. This would enable a one-pot reaction with both the flap primer cleavage by FEN and adaptor ligation occurring simultaneously. To validate our choice of ligase, we measured the ligation efficiency of Taq ligase at 65 °C and compared it to that of other ligases, with the reaction performed at the reported optimal temperature of the enzyme: T4 DNA ligase at 21 °C and T4 RNA ligase at 37 °C. We used a synthetic flap oligo and the dsDNA adaptor as the substrate and performed ligation for 30 min. The ligated product was detected by the Cas12-sgRNA complex, with fluorescence signals measured after 10 min or 30 min of incubation at 37 °C (Fig. 3b). Among the three ligases tested, Taq DNA ligase exhibited the highest fluorescence signal within 10 min of incubation with Cas12-sgRNA, which was comparable to the signal of the preligated product (Fig. 3c). This result demonstrates the superiority of Taq ligase over other ligases. Thus, Taq ligase was used as the ligase of choice for FELICX.

Next, we optimized the one-pot FEN + Taq ligase reaction step by varying the concentration of FEN and the reaction incubation time at 65 °C. As the reaction requires a FEN concentration with high specific and minimal nonspecific activity (Fig. 2c), we hypothesized that a similar trend would also be observed for the FEN + Taq ligase reaction. Fig. 3d shows that the optimal FEN concentration was 10 nM, as it produced the strongest fluorescence signal. Meanwhile, lower and higher FEN concentrations yielded weaker signals, validating our hypothesis. At low concentrations of FEN, fewer flap products are formed, resulting in weaker fluorescence signals. However, at high FEN concentrations, the nonspecific activity of FEN may yield flap products of shorter length that do not anneal to the dsDNA adaptor due to the high reaction temperature or are not recognized by the Cas12-sgRNA complex after ligation due to incomplete hybridization of the sgRNA to the ligated product. Additionally, the fluorescence signal improved with increased incubation time, with 4 h of incubation yielding the strongest signal. To further strengthen the fluorescence signal, we increased the concentration of both the Cas12-sgRNA complex and the DNA reporter, which led to a significant increase in the specific signal (Fig. S6). We also evaluated a modified sgRNA, extended at the 3′ end with ssDNA, which has previously been reported to increase the *trans*-cleavage activity of LbCas12a (Nguyen et al., 2020). However, no improvement in activity was observed compared to that of the unmodified sgRNA (Fig. S7). Using these optimized conditions, we evaluated the detection limit of DNA and RNA by FELICX to determine whether signal amplification by FEN and Cas12 was sufficient for the sensitive detection of nucleic acids. For this, we used the partial *orf1ab* DNA or RNA substrates of SARS-CoV-2 spiked into purified total DNA or RNA from HEK293T cells, respectively, to simulate clinical samples. Despite a prolonged incubation of 4 h at 65 °C, only up to 100 pM target was detected by FELICX when both substrates were tested (Fig. 3e and f). This indicates the need for further improvements in the sensitivity of FELICX. Although this detection limit is similar to that observed with FEN alone (Fig. 2d and e), the fluorescence signals observed with FELICX were significantly higher compared to FEN alone, indicating signal amplification by Cas12.

Previously reported nucleic acid detection methods have incorporated isothermal nucleic acid amplification techniques, such as loop-mediated isothermal amplification (LAMP) and recombinase polymerase amplification (RPA), to improve detection sensitivity (Broughton et al., 2020; Kellner et al., 2019). We attempted to amplify the target nucleic acids by LAMP, a commonly used nucleic acid amplification method performed at 65 °C, followed by FELICX to detect the partial *orf1ab* DNA of SARS-CoV-2 spiked into purified total DNA from HEK293T cells. However, *orf1ab* DNA was not detected despite extensive assay optimization (Supplementary result: Nucleic acid detection with LAMP + FELICX).

As nonspecific amplification was observed by LAMP with the six primers used in the reaction, we hypothesized that using alternate amplification methods requiring fewer primers, such as RPA and helicase-dependent amplification (HDA), might eliminate the formation of nonspecific products, improving the sensitivity of target detection. Between these two methods, we chose HDA because its working temperature (65 °C) (An et al., 2005) is the same as the temperature of the FEN + Taq ligation step, simplifying the operation of HDA + FELICX. When FELICX was coupled with HDA, we detected six copies/μL (10 aM) of *orf1ab* and two copies/μL (3.5 aM) of the *E. coli* genome in two out of three biological samples (Fig. 3g and h), a significant improvement compared to LAMP, particularly for *orf1ab* detection. This validates our hypothesis that the presence of fewer primers in the nucleic acid amplification step can prevent nonspecific product formation and increase target yield, greatly improving its subsequent detection.

2.4. Integration of a lateral flow detection system into FELICX

Based on the finding that HDA + FELICX enabled nucleic acid detection, we next sought to integrate a lateral flow system into FELICX for signal detection to eliminate the need for a fluorescence reader. We used PCRD Flex lateral flow strips that can detect two different oligos with conjugated biotin and either FAM or digoxigenin (Fig. 4a). In the final step of FELICX, the Cas12-sgRNA complex cleaves the DNA reporter in the presence of its substrate. To make use of this cleavage activity for the lateral flow strips, we replaced the DNA fluorescence reporter with probes for PCRD Flex. In the presence of the substrate, the Cas12-sgRNA complex should cleave the probe, resulting in the disappearance of the corresponding band on the lateral flow strip (Fig. 4b). Thus, a positive signal for the target nucleic acid is represented by the absence of the band on the lateral flow strip.

We used the partial *orf1ab* DNA as the target to verify the functionality of the lateral flow strips with FELICX. As the sensitivity of the lateral flow strips is poorer than that of the fluorescence reader, we scaled up the HDA reaction volume from 10 μL to 25 μL. Since high variability and weaker signals were observed when the unpurified HDA product was used for FELICX (Fig. 3g and h), we also included a nucleic acid purification step after HDA. For purification, we used the ChargeSwitch PCR Clean-Up Kit, which is based on functionalized magnetic

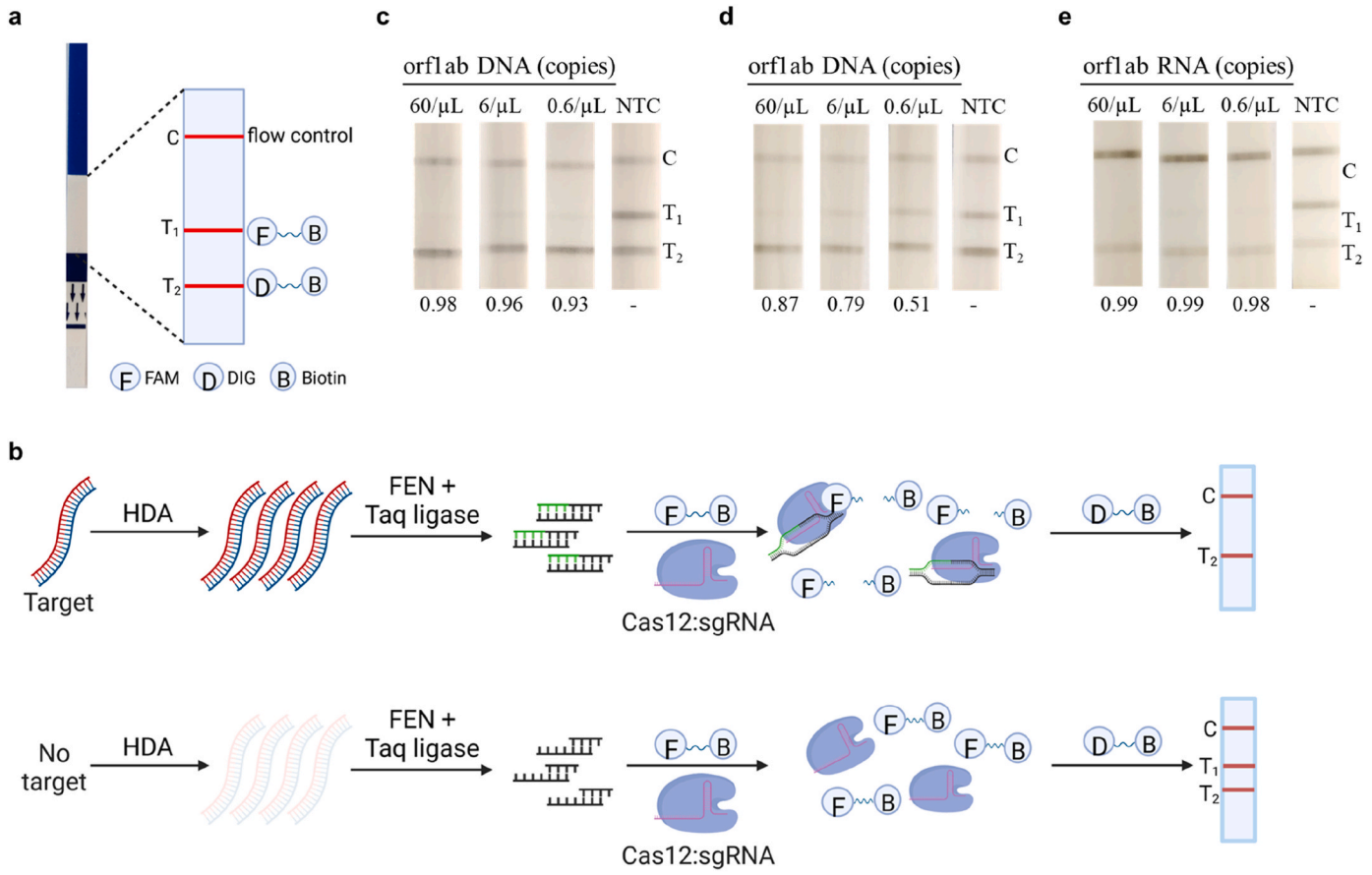


Fig. 4. Combining FELICX with lateral flow strips for nucleic acid detection. (a) Schematic of the lateral flow strip used in this study. Test line T_1 corresponds to the reporter with FAM and biotin, while T_2 corresponds to the reporter with digoxigenin (DIG) and biotin. C is the lateral flow control. (b) Schematic of nucleic acid detection using HDA + FELICX along with lateral flow strips. Lateral flow output in the presence and absence of the target in the sample is depicted. (c) Lateral flow for the detection of *orf1ab* DNA spiked into HEK293T total DNA. HDA was performed for 1 h in a 25 μL reaction followed by rapid purification, FEN + Taq reaction for 1 h (total volume 20 μL), and Cas12-sgRNA reaction for 30 min (total volume 27 μL). In this experiment, only T_1 was used. The numbers below the strips show the fold change in the T_1 band intensity compared to NTC. (d) Same as (c) with the HDA, FEN + Taq, and Cas12-sgRNA reactions performed for 20 min each. The numbers below the strips show the fold change in the T_1 band intensity compared to NTC. (e) Lateral flow for the detection of *orf1ab* RNA spiked into HEK293T total RNA. HDA was performed for 45 min in a 25 μL reaction followed by rapid purification, FEN + Taq reaction for 20 min (total volume 20 μL), and Cas12-sgRNA reaction for 20 min (total volume 27 μL). Only T_1 was used in the experiment. The numbers below the strips show the fold change in the T_1 band intensity compared to NTC.

beads that bind to either DNA/RNA. The kit requires only a magnet and can be used to rapidly purify nucleic acids (~5 min). When coupled with HDA and subsequent purification, we detected up to 0.6 copies/μL (1 aM) *orf1ab* DNA spiked into purified HEK293T DNA using FELICX, as indicated by the disappearing T_1 band in the lateral flow strip (Fig. 4c). The total time for detection was 2.5 h, including 1 h of HDA, 1 h of FEN + Taq ligation, and 30 min of the Cas12-sgRNA reaction. We next checked if the time taken for HDA + FELICX could be reduced to enable the rapid detection of the target DNA. There was no loss of sensitivity when the time for HDA + FELICX was reduced to 60 min (20 min each of HDA, FEN + Taq ligation, and Cas12-sgRNA) (Fig. 4d), demonstrating the robustness of HDA + FELICX.

Having confirmed the applicability of this method for rapid and sensitive detection of DNA, we next attempted to use HDA + FELICX to detect RNA targets. As the HDA reaction mixture lacks a dedicated reverse transcriptase, we used the WarmStart RTx reverse transcriptase due to its optimal temperature of 65 °C and similar buffer requirements as HDA. As RTx has not been used previously with HDA, we evaluated the functioning of RTx + HDA in a one-step (one-pot RTx + HDA) or two-step (sequential RTx and HDA) reaction to determine whether RTx interferes with the HDA reaction. There was no difference observed between the reactions (Fig. S10), leading us to choose the one-step RTx + HDA due to its lower complexity. We performed RTx + HDA followed by FELICX to detect *orf1ab* RNA spiked into purified HEK293T RNA, detecting 0.6 copies/μL RNA (Fig. 4e) in the process. It took ~90 min in total to detect the RNA (45 min for RTx + HDA, 20 min for FEN + Taq ligation, and 20 min for Cas12-sgRNA). These results demonstrate that HDA + FELICX can detect both DNA and RNA using lateral flow strips with similar sensitivities in 60 min and 90 min, respectively.

2.5. Demonstration of the versatility of FELICX

In the previous section, we showed that FELICX in combination with HDA can be used to detect nucleic acids rapidly with high sensitivity. We next attempted to broaden the range of potential applications of FELICX by using it to detect SNPs. Detecting SNPs is important for disease diagnosis and treatment, as well as for identifying pathogen variants. FEN can be used to distinguish between SNPs by designing the flap and invading primers such that the one base-pair overlap between the primers falls at the SNP position (Fig. 5a). If there is an SNP in the target, the absence of overlap between the flap and the invading primers will abolish the activity of FEN. Thus, the absence or presence of the SNP in the target sample can be confirmed by probing the sample with flap primers specific to the wild type and the variant target sequence (Fig. 5b). As a proof-of-concept, we used FELICX to distinguish between the receptor-binding domain in the spike protein of wild-type SARS-

CoV-2 and its variant carrying the T478K mutation, which is found in the Delta and Omicron variants of the virus (Kumar et al., 2022). Flap primers, namely, the WT and mut probes, specific to the wild-type (WT) sequence and the variant, respectively, were designed and used to probe both targets. In the case of the WT target, after FELICX, there was an ~2.5-fold higher fluorescence signal with the WT probe compared to the mut probe (Fig. 5c). In contrast, the variant target with the T478K mutation showed an ~2.5-fold higher fluorescence signal with the mut probe than with the WT probe. Although the difference between the WT and T478K variants was only a single base pair (with the ACG codon changed to AAG), FELICX easily detected the SNP, as indicated by the opposite trend in the fluorescence signal observed for the WT and the variant sequence.

Furthermore, we made use of the PCRD Flex strips that can detect two different oligos for SNP detection, with each test line corresponding to either the WT or mut probes. For this, we replaced the fluorescent DNA reporter with a FAM-biotin reporter for the WT probe and a DIG-biotin reporter for the mut probe (Fig. 5b). Similar to the result shown in Fig. 5c, the WT sample showed a positive signal with the WT probe, as indicated by the disappearance of the band corresponding to this probe (Fig. 5d and e). For the T478K variant, the band corresponding to the mut probe disappeared, indicating that a positive signal was obtained with this probe. This demonstrates that FELICX can be used to identify SNPs in the target with ease by carefully designing the flap primer and using the PCRD Flex strips to detect the multiple signals generated.

Beyond SARS-CoV-2, we determined whether FELICX can be used to detect other pathogens of interest in more complex samples. First, we used FELICX to detect EBV, which causes infectious mononucleosis and is associated with autoimmune diseases, nasopharyngeal carcinoma (NPC), and other neoplasms (AbuSalah et al., 2020). We used C666-1, an NPC cell line and a natural host of the virus (Cheung et al., 1999). The EBV-negative HK-1 NPC cell line (Daker et al., 2016) was also included in the analysis, with the housekeeping gene *gapdh* used as the internal control for assay functionality. To lyse the mammalian cells and release genetic material, a 10 min incubation at 65 °C in an SDS-based lysis buffer and purification with a ChargeSwitch PCR Clean-Up kit were included before HDA. Following this, RTx + HDA and FELICX were performed to detect EBV and *gapdh* in the samples. Using these conditions, we detected both EBV and *gapdh* at levels as low as 0.6 cells/μL of C666-1 (Fig. 6a and S11, top panel), demonstrating highly sensitive EBV detection by HDA + FELICX. The detection of only the *gapdh* signal in HK-1 cells suggests that the assay was functional and that HK-1 was truly negative for the virus. Moreover, the sensitive detection of the target in whole cells using HDA + FELICX further validated the robustness of our method.

Next, we used FELICX to detect *K. pneumoniae*, the most common nosocomial pathogen. Nosocomial infections are a major source of patient complications worldwide (Low et al. 2021). *K. pneumoniae* is known to be a causative agent for neonatal sepsis, pneumonia, surgical wound infection, and cystitis (Navon-Venezia et al., 2017; Wyres et al., 2020). In addition to its wide prevalence, *K. pneumoniae* is also a major source of antibiotic resistance genes, particularly those encoding carbapenemases (Munoz-Price et al., 2013). Detecting the pathogen in clinical samples and definitively identifying its antibiotic resistance status is therefore essential for guiding infection treatment. Thus, we used HDA + FELICX to detect the carbapenemase resistance gene (bla_{KPC}) in pathogenic *K. pneumoniae* DSM 2026 bacterial cells spiked into whole HK-1 cells. As an internal control, we used the hemolysin gene (*khe)*, which is present in all *K. pneumoniae* isolates (Hartman et al., 2009). RTx was omitted from the assay, as we aimed to detect only the genomic copies of target genes. Using similar conditions as those described for EBV detection, we detected bla_{KPC} and *khe* in up to 0.6 c.f.u./μL K. *pneumoniae* DSM2026 (Fig. 6b and S11, bottom panel). No signal was observed for either gene in HK-1 cells alone. As RTx was not used in this assay, only the copies of the genes in the *K. pneumoniae* DSM2026 genome were detected, underscoring the assay's high detection sensitivity.

Finally, we tested FELICX for cell-free nucleic acid detection in serum as a potential cancer biomarker. Detecting extracellular DNA or RNA in bodily fluids has been proposed as a noninvasive and cost-effective method for early cancer diagnosis (Tzimagiorgis et al., 2011). *SCGB2A2* (mammaglobin A) RNA was previously reported to be a biomarker for hormone receptor-positive (HR+) breast cancer, with transcripts in the blood samples observed only in cancer patients (Larson et al., 2021). To simulate patient samples, we spiked *SCGB2A2* RNA into fetal bovine serum (FBS) at varying concentrations and used FELICX with RTx + HDA to detect the transcript. After purifying the RNA from FBS using the ChargeSwitch PCR Clean-Up kit, we detected the transcript at up to 12 copies/μL (20 aM) (Fig. 6c). In summary, FELICX can be used to detect nucleic acids with high specificity and sensitivity in several clinical settings, including pathogen detection, antibiotic resistance identification, distinguishing between wild-type sequences and their variants with SNPs, and finally, cancer diagnostics.

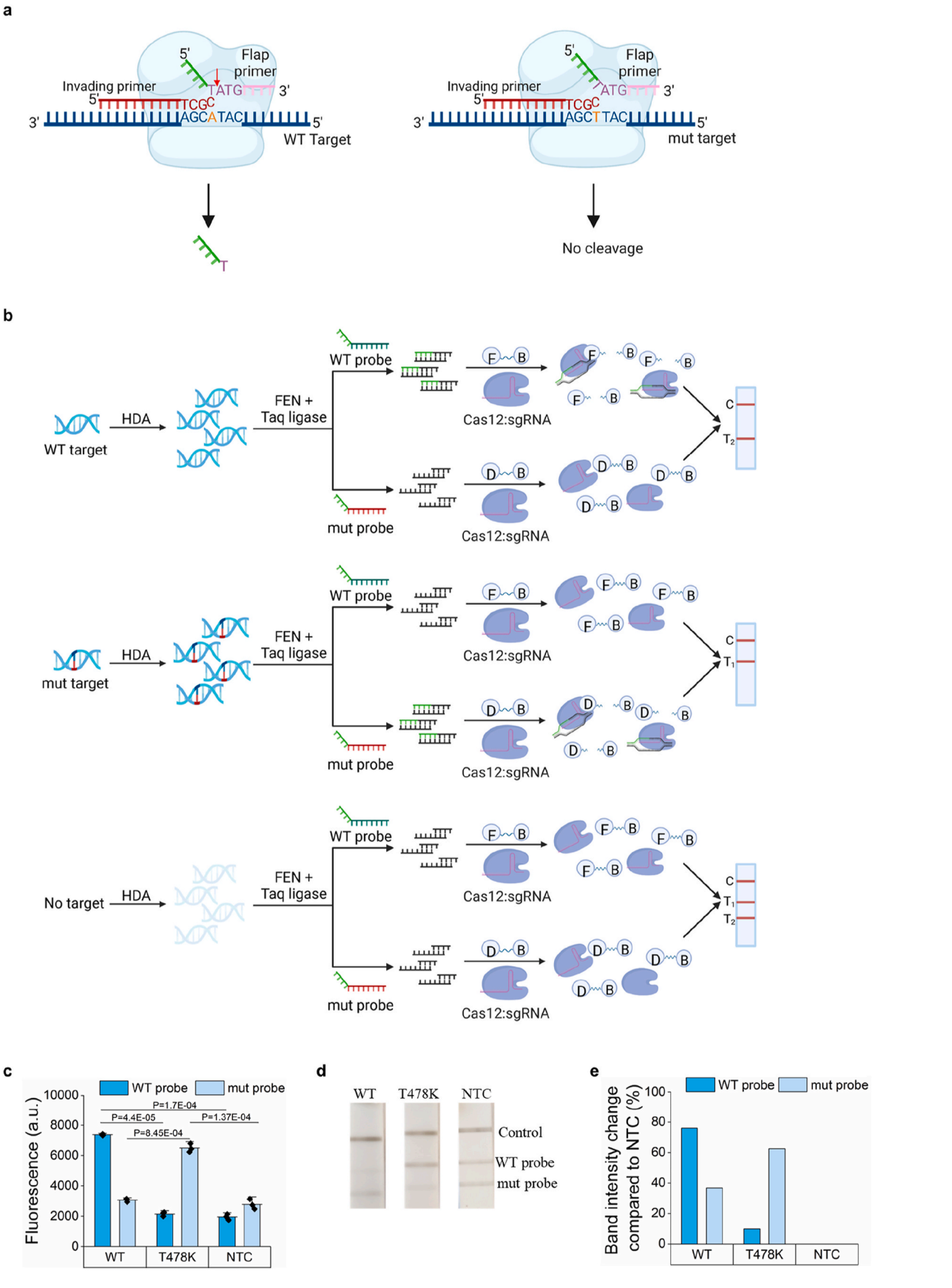
3. Discussion

Rapid, sensitive, and accurate nucleic acid detection is the hallmark of CRISPR-based technologies, especially in point-of-care settings. Although promising, existing CRISPR-based diagnostic tools suffer from several drawbacks, such as PAM dependence, off-target activity, and extensive sgRNA optimization. Further improvements are needed before CRISPR-Cas systems can be leveraged to fulfill the increasing demand for robust diagnostics.

In this report, we have described the development of FELICX, a highly sensitive and specific method for nucleic acid detection (Fig. 1). We showed that by using FELICX, comprising Tth pol v2, Taq ligase, and Cas12-sgRNA, up to 15 copies (0.6 copies/μL in a 25 μL reaction) of *orf1ab* DNA and RNA of SARS-CoV-2 could be detected in 60 min and 90 min, respectively, using simulated samples (Fig. 4g and h). For comparison, the sensitivity of previously reported CRISPR-Ca12-based technologies are as follows: 20 copies for DETECTR (Broughton et al., 2020), 50 copies for VaNGuard (Ooi et al., 2021), and 100 copies for STOPCovid.v2 (Joung et al., 2020).

In FELICX, the target nucleic acid is probed directly by FEN, which offers several advantages. First, it enables the single base-pair resolution of the substrate, which has wide-ranging applications, from disease diagnosis to pharmacogenomics, along with distinguishing between pathogen variants, as shown in the recent COVID-19 pandemic (Cyranoski 2021; Kim and Misra, 2007). In previously reported CRISPR-based technologies, Cas12 was used to directly probe the target and, in some cases, detect SNPs (Huang et al. 2021; Teng et al., 2019). However, this often requires extensive optimization and synthesis of multiple sgRNAs due to the high mismatch tolerance of the CRISPR-Cas system. In comparison, SNP detection by FEN is easier to achieve, with the only requirement being a pair of DNA oligos overlapping at the SNP position. Second, the use of FEN enables the probing of the target in a PAM-independent manner, unlike Cas12, which is constrained by the need for a PAM adjacent to the sgRNA-binding site. Although Cas12 variants have been engineered to loosen the PAM constraint (Collias and Beisel, 2021; Tóth et al., 2020), complete independence has not yet been achieved. Third, FELICX does not require sgRNA activity optimization since the dsDNA adaptor and the flap sequence remain constant irrespective of the target sequence, eliminating the need to design new sgRNAs for new targets. Thus, FELICX can overcome the shortcomings of CRISPR-based technologies, providing a useful alternative to existing methods.

Moreover, the design of FELICX enables the method to be easily and rapidly repurposed for various applications. Reprogramming FELICX to detect novel targets only requires the optimization of oligos for isothermal application, as well as the flap and invading primers. This facilitates the deployment of FELICX for nucleic acid detection within 24 h after the genetic sequence and material are made available, such as



(caption on next page)

Fig. 5. SNP detection using FELICX. (a) Schematic showing the cleavage of the flap primer by the FEN in the case of the wild-type (WT) target, whereas no flap primer cleavage was observed for the target with the SNP. The cleavage site of the flap primer is marked by the red arrow. The SNP position is in orange. The last nucleotide of the invading primer is mismatched with the target, an essential feature for the FEN cleavage reaction. (b) Detection of the WT target, target with mutation or no target with FELICX and the corresponding lateral flow strip pattern observed in each case. (c)-(e) Detection of the WT receptor binding domain sequence of SARS-CoV-2 or its variant (T478K) by FELICX using WT and mut probes. (c) shows the fluorescence signals, whereas (d) shows the lateral flow result after FELICX was performed on pre-amplified substrates using both probes. Pre-amplification was performed through PCR, followed by DNA purification, to ensure that an equal mass of both WT and mutated DNA was used for accurate comparison. The FEN + Taq reaction was performed for 60 min (total volume 20 μL), and the Cas12-sgRNA reaction was performed for 30 min (total volume 27 μL). In (c), the data represents the mean ± SD (n = 3 biological repeats). The p value < 0.05 compared to NTC are provided, calculated using a two-sample *t*-test. (e) Percentage change in band intensity corresponding to WT and mut probes compared to NTC in (d). NTC - no target control.

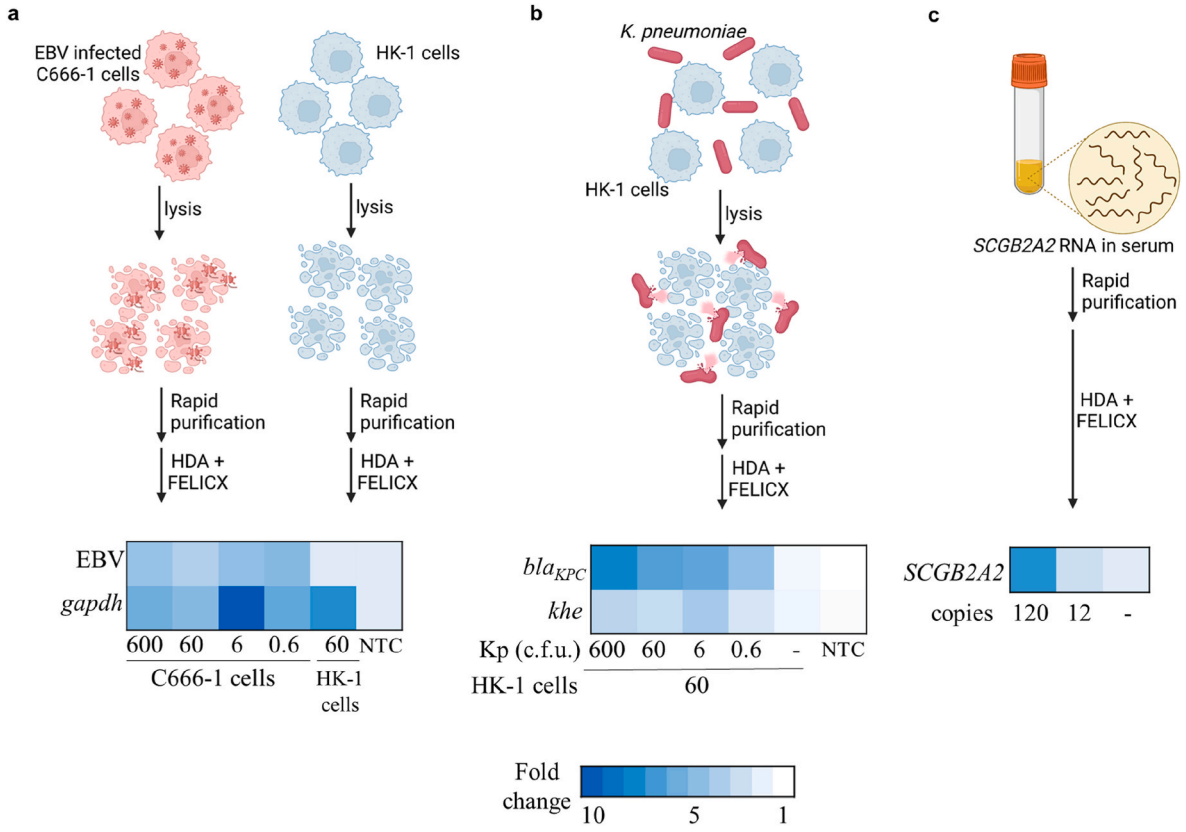


Fig. 6. Demonstration of the versatility of FELICX. FELICX was used to detect targets in more complex samples, such as whole bacterial and mammalian cells and serum. Fold change in the fluorescence signal for the detection of (a) EBV and *gapdh* in whole C666-1 and HK-1 cells, (b) bla_{KPC} and *khe* in *K. pneumoniae* (Kp) cells spiked into HK-1 whole cells and (c) *SCGB2A2* RNA spiked into FBS. Samples were lysed and rapidly purified as described in the Methods. HDA was performed for 1 h in a 10 μL reaction, FEN + Taq ligase reaction for 1 h (total volume 20 μL), and Cas12-sgRNA reaction for 30 min (total volume 27 μL). NTC - no target control.

for a new pathogen or variant (Fig. S12). This was exemplified when we used FELICX to detect EBV, an antibiotic resistant-*K. pneumoniae* strain, and a breast cancer biomarker (Fig. 6).

Despite these advantages, applying FELICX in point-of-care testing may require further improvements. Currently, HDA + FELICX requires two temperatures: 65 °C for HDA, FEN, and Taq ligase, and 37 °C for the Cas12-sgRNA reaction. However, thermostable engineered Cas12 enzymes that have an optimal temperature of 60–65 °C have been reported (Ooi et al., 2021). Incorporating this engineered Cas12 into FELICX will enable the isothermal detection of the desired target and simplify its operation, as seen in previous studies (Malcı et al., 2022; Woo et al., 2020; Yoon et al., 2022). Eliminating the isothermal amplification step and directly detecting the nucleic acid by FELICX may also be made feasible by improving the FEN activity of Tth pol v2 through mutagenesis. The release of the substrate after the cleavage of the flap primer has been reported to be the rate-limiting step for FEN (Tarantino et al., 2015). Thus, mutating the substrate-binding region of Tth pol combined with high-throughput screening is likely to yield superior FEN variants, as seen for other proteins (D'Ambrosio et al., 2020). A previously reported strategy for detecting FEN activity using CRISPR-Cas12 (Song et al., 2022) may also aid in FEN mutant screening. Another potential method for enhancing the signal generated by FEN is to provide multiple sets of flap and invading primers that bind to different locations on the target DNA or RNA. By keeping the 5′-flap of the flap primers constant, the use of multiple flap primers at different loci will result in a higher number of cleaved flaps, subsequently increasing the speed and sensitivity of FELICX. In the future, an optimized FELICX will be used on a wide variety of clinical samples to validate its specificity and sensitivity, which would be vital to accurately assess its true potential as a point-of-care nucleic acid diagnostic method.

4. Conclusion

In this work, we developed FELICX for the detection of nucleic acids and SNPs. FELICX significantly improves upon existing CRISPR-based diagnostic methods through its ability to rapidly detect nucleic acids with single base-pair resolution in a PAM-independent manner. This was achieved by using a mutated flap endonuclease to detect the target

followed by signal amplification using CRISPR-Cas12. Due to the sequence-independent activity of the flap endonuclease, FELICX also overcomes the need for extensive gRNA optimization for new targets. Thus, FELICX is a promising next-generation CRISPR-based technology that can easily be customized to enable nucleic acid detection for a wide range of applications.

5. Methods

5.1. Bacterial strains, plasmids and oligonucleotides used in the study

E. coli TOP10 was used as the cloning host and *E. coli* BL21(DE3) was used for protein expression. Both bacterial strains were grown in Luria-Bertani (LB) broth at 37 °C with shaking at 220 rpm unless stated otherwise.

pET28b was used as the cloning vector to express the proteins in *E. coli* BL21(DE3). Cas12 was obtained from pMBP-LbCas12a, which was a gift from Jennifer Doudna (Addgene plasmid # 113431). The Tth pol (GenBank accession no. WP_011228405), hFEN1 (GenBank accession no. NP_004102), MjaFEN (GenBank accession no. WP_010870964) and T5 exo (GenBank accession no. YP_006958) sequences were codon optimized for expression in *E. coli* and synthesized as gblocks from Integrated DNA Technologies (IDT).

The sequence of the oligos and primers for LAMP, HDA and FEN (flap and invading primers) are provided in Tables S1–4.

5.2. Protein purification

All proteins were purified by using the His tag attached at their C-termini. For Cas12 purification, *E. coli* BL21(DE3) (pET28b-Cas12) was grown overnight in Luria-Bertani (LB) broth supplemented with kanamycin (50 μg/mL). After overnight growth, the culture was diluted 10-fold in Terrific Broth supplemented with kanamycin and grown at 37 °C until the OD_{600} reached ~0.3–0.4. Following this, 100 mM IPTG was added to the cultures and grown further for 24 h at 23 °C. The cells were collected by centrifugation and resuspended in lysis buffer (50 mM Tris-Cl (pH 8), 300 mM NaCl, EDTA-free protease inhibitor tablets). The cells were lysed using a homogenizer by passing the cells at 23,000 bar 5–10 times. The lysate was centrifuged, and the supernatant was subjected to protein purification using a HisTrap HP column connected to an FPLC instrument. Elution was performed with lysis buffer supplemented with 1 M imidazole, following a gradient run over 2 h. Different fractions were collected and run on an SDS-PAGE gel to confirm protein purification. The purified protein was washed with lysis buffer without protease inhibitor tablets to remove imidazole and then concentrated and flash frozen for storage.

FEN enzyme purification was performed in the same manner with slight modifications. The growth medium for protein expression was changed to LB, and the protein was expressed at 37 °C for 4–5 h. Cell lysis was performed using Y-PER (Thermo Fisher), and the soluble proteins were purified using Ni-NTA resin in a PD-10 column. Elution was performed using lysis buffer supplemented with 50 mM, 100 mM, 200 mM, and 500 mM imidazole. Purified proteins (final concentration 1 μM) were stored in a buffer comprising 50% glycerol, 0.1 mM EDTA, 1 mM DTT, and 0.1% Triton-X-100 at −20 °C.

5.3. FEN activity assay

The activity of various FEN enzymes was evaluated in an isothermal reaction comprising reaction buffer RB (50 mM Tris-Cl (pH 8), 100 mM NaCl, 10 mM $MgCl_2$), 100 nM flap primer, 20 nM invading primer, 0.2% Triton-X-100, 50 nM purified FEN enzyme (unless otherwise stated), and 1 nM target template (unless otherwise stated) in a 20 μL reaction incubated at 65 °C for the appropriate time. When using the flap primer with a conjugated fluorophore and quencher, the fluorescence (ex: 485 nm, em: 535 nm) was measured every 5 min.

5.4. Ligation assay

To ligate the synthesized flap oligo to the dsDNA adaptor, the latter was formed by annealing the 5' p adaptor and ds convertor (final concentration 200 nM) in 1X RB. For this, the reaction mixture was heated to 98 °C and cooled to room temperature at 0.1 °C/s in a thermocycler. The ligation was carried out by adding 1X RB, 5 nM dsDNA adaptor, 5 nM flap oligo, and the appropriate additive and co-factor depending upon the ligase used. For T4 DNA ligase and T4 RNA ligase (NEB), 1 mM DTT and 1 mM ATP (NEB) were added to the reaction. For Taq DNA ligase (NEB), 1 mM NAD (Sigma Aldrich) and 10 mM DTT were added to the reaction. The amounts of ligase used were 5 U of T4 DNA ligase, 10 U of T4 RNA ligase, and 80 U of Taq DNA ligase. The incubation temperatures were 22 °C for T4 DNA ligase, 37 °C for T4 RNA ligase, and 65 °C for Taq ligase.

5.5. Cas12-sgRNA reaction

The Cas12-sgRNA complex was formed by incubating 3.75 μL of purified Cas12 (100 μM) and 0.3125 μL of 1 mM sgRNA in 2 μL of 1X RB with 20 mM DTT (RB-DTT) made up to a final volume of 20 μL with nuclease-free water. The incubation was performed at 37 °C for 30 min. Following this, the Cas12-sgRNA complex was diluted to 375 μL with water to achieve a final Cas12:sgRNA concentration ratio of 1 μM:0.833 μM.

For the reaction with the Cas12-sgRNA complex, 3 μL of the complex formed as above, 4 μL of the fluorophore-quencher reporter (1 μM), and 0.7 μL of 1X RB were added to the reaction and incubated at 37 °C, with fluorescent measurements taken every 3 min (ex: 485 nm, em: 535 nm). For the data in Figures S5, S7 and S8, 1.5μL of Cas12-sgRNA complex and 2 μL of the fluorophore-quencher reporter were used.

5.6. LAMP assay

To perform LAMP, a Warmstart LAMP kit (DNA and RNA) from NEB was used, and the assay was performed according to the manufacturer's instructions. LAMP primers were designed using either PrimerExplorer v5 or the NEB LAMP primer design tool. To biotinylate the LAMP product for subsequent purification with streptavidin agarose beads, the primers FIP, BIP, LF, and LB were biotinylated at the 5′-end. After LAMP, 10 μL of DNA product was purified by adding an equal volume of Pierce Streptavidin Agarose resin resuspended in B&W buffer (10 mM Tris-Cl (pH 7.5), 1 mM EDTA and 2 M NaCl). The sample was diluted further by adding 30 μL of 0.5X B&W buffer and incubating the mixture for 30 min at room temperature for biotin-streptavidin conjugation. After 30 min, the supernatant was removed after the beads settled. These beads were subsequently used for FELICX.

5.7. HDA assay

HDA was performed using the IsoAmp II Universal tHDA kit from NEB. The assay was performed according to the manufacturer's instructions, with primers designed using the PrimerQuest tool from IDT. For all HDA reactions, $MgSO_4$ (4 mM), NaCl (40 mM) and the appropriate primers (200 nM) were used. After assay completion, the DNA product was used directly for FELICX or purified using the ChargeSwitch PCR Clean-Up kit from Invitrogen followed by FELICX. When RNA was used as the template, 0.25 μL Warmstart RTx (NEB) was added to every 10 μL of HDA assay mix.

5.8. FELICX

In the first step of FELICX, amplified DNA was added to the FEN + Taq mix comprising of: 2 μL of flap primer (1 μM), 0.4 μL of invading primer (1 μM), 0.5 μL of dsDNA adaptor (200 nM, as described in the ligation assay), 2 μL of RB-DTT buffer, 1 μL of Triton-X-100 (2%), 1 μL of

NAD (20 mM), 0.5–1 μL of FEN, and 0.5 μL of Taq ligase, made up to a final volume of 20 μL with nuclease-free water. The reaction was carried out at 65 °C for the appropriate duration. Following this, the reaction mixture was added to the Cas12-sgRNA mix, comprising 3 μL of Cas12-sgRNA complex (as described for the Cas12-sgRNA reaction), 4 μL of FAM-IBFQ reporter probe (1 μM), and 0.7 μL of RB-DTT and incubated at 37 °C with the fluorescence (ex: 485 nm, em: 535 nm) measured in a microplate reader every 3 min.

For the lateral flow strips, the FAM-IBQF reporter was replaced with 0.25 μL of FAM-Bio reporter (1 μM) or 0.1 μL of DIG-Bio reporter (1 μM). Following Cas12 cleavage, the reaction mix was run on PCRD Flex strips from Abingdon Health according to the manufacturer's instructions. Band intensity was quantified using ImageJ.

5.9. SNP detection

To detect the T478K mutation in the receptor-binding domain (RBD) of SARS-CoV-2, the mutation was introduced in pCDNA3-SRARS-CoV-2-S-RBD-Fc, which carries the RBD region (~1.5 kB) of the virus, by overlap PCR using the primers spike-T478K–F/R. After confirming mutagenesis by sequencing, the wild-type and mutated RBD regions were PCR amplified using the primers spike-F/R and an equal amount of plasmid. Following amplification, 50–150 ng of purified PCR product was used as the template for FELICX, which was performed as previously described with slight modifications. The volume of the flap primers (WT and mut probes) was increased to 3 μL (final concentration 150 nM). Both templates were analyzed with the WT and mut probes. In the case of the lateral flow strips, the FAM-Bio reporter was used in the Cas12-sgRNA cleavage reaction for the WT probe samples and the DIG-Bio reporter was used for the mut probe samples.

5.10. Detection of genes in mammalian cells

The C666-1 cell line was kindly provided by Dr Joshua Tay from the Department of Otolaryngology, Yong Loo Lin School of Medicine, National University of Singapore, and the HK-1 cell line was a gift from A/Prof Zhong Yong Liang from the Department of Microbiology & Immunology, Yong Loo Lin School of Medicine, National University of Singapore. Both cell lines were grown in Gibco BenchStable RPMI 1640 (Life Technologies, Catalog # A4192301) supplemented with 10% FBS (Biowest, Catalog # S181H) and 1% penicillin-streptomycin (Gibco, Catalog # 15140122) at 37 °C in 5% CO_2. After reaching 70–80% confluency, the cells were trypsinized and washed with RPMI, and cell numbers were counted using a Luna cell counter. A fixed number of C666-1 or HK-1 cells were lysed by incubation in lysis buffer (10 mM Tris-Cl (pH 7.5), 200 μg/mL proteinase K, 0.1% SDS, 2 mM $CaCl_2$) at 65 °C for 10 min. After lysis, the genetic material was purified using a ChargeSwitch PCR Clean-Up kit and subjected to FELICX as described above. The fluorescence measured after 30 min of the Cas12-sgRNA reaction was then reported.

5.11. Detection of genes in K. pneumoniae

An overnight culture of *K. pneumoniae* DSM 2026 grown in LB broth at 37 °C in shaking conditions was diluted to obtain the required c.f.u. based on the formula $OD_{600} = \sim 10^8$ c.f.u. HK-1 cells were grown in Gibco BenchStable RPMI 1640 (Life Technologies, Catalog # A4192301) supplemented with 10% FBS (Biowest, Catalog # S181H) and 1% penicillin-streptomycin (Gibco, Catalog # 15140122) at 37 °C in 5% CO_2. After reaching 70–80% confluency, the cells were trypsinized and washed with RPMI, and cell numbers were counted using a Luna cell counter. Simulated clinical samples were prepared by mixing *K. pneumoniae* with HK-1 cells, as needed, and lysing the samples by incubation in lysis buffer (10 mM Tris-Cl (pH 7.5), 200 μg/mL proteinase K, 0.1% SDS, 2 mM $CaCl_2$) at 65 °C for 10 min. After lysis, the genetic material was purified using a ChargeSwitch PCR Clean-Up kit and subjected to FELICX as previously described. The fluorescence after 30 min of the Cas12-sgRNA reaction was then reported.

5.12. Detection of cancer biomarkers

To prepare the template, overlapping primers (scgb1-F, scgb2-R, scgb3-F and scgb4-R) were designed and PCR amplified with scgb2a2-T7-F and scgb2a2-R. The final construct incorporates a T7 promoter at the 5′-end of *SCGB2A2,* enabling *in vitro* transcription by the Hiscribe T7 High Yield RNA Synthesis kit (NEB). The transcribed product was purified by a Monarch RNA Clean-Up kit (NEB) and used for FELICX. To simulate clinical samples, RNA was quantified and spiked into Fetal Bovine Serum (FBS) South America, Heat Inactivated (Biowest, Catalog # S181H). The simulated samples were processed with a ChargeSwitch PCR Clean-Up kit to purify the spiked RNA followed by HDA with RTx and FELICX, as previously described. The fluorescence after 30 min of the Cas12-sgRNA reaction was then reported.

CRediT authorship contribution statement

Nikhil Aggarwal: Conceptualization, Methodology, Investigation, Formal analysis, Writing – original draft. **Yuanmei Liang:** Methodology, Investigation, Writing – review & editing. **Jee Loon Foo:** Formal analysis, Writing – review & editing. **Hua Ling:** Formal analysis, Writing – review & editing. **In Young Hwang:** Conceptualization, Methodology, Formal analysis, Writing – review & editing. **Matthew Wook Chang:** Conceptualization, Methodology, Formal analysis, Writing – review & editing, Supervision, Funding acquisition.

Declaration of competing interest

N.A., J.L.F., H.L., I.Y.H. and M.W.C have filed a patent application through the National University of Singapore based on the work described in this manuscript. The remaining authors declare no competing interests.

Data availability

Data will be made available on request.

Acknowledgements

We thank Kwok Soon Wun and Kamila Isabelle Alabado Navarro for the comments made on the manuscript. This work was supported by the Summit Research Program of the National University Health System (NUHSRO/2016/053/SRP/05, M.W.C.), Investigatorship of the National Research Foundation of Singapore (NRF-NRFI05-2019-0004, M.W.C.), ISF-NRF Joint Programme of the National Research Foundation of Singapore (NRF2019-NRF-ISF003-3208, I.Y.H.) and NUS Medicine Synthetic Biology Translational Research Program (NUHSRO/2020/077/MSC/02/SB, M.W.C). This work used the resources of the Singapore BioFoundry, a bio-manufacturing research facility located at the National University of Singapore. All schematics were created with Biorender.com.

Appendix A. Supplementary data

Supplementary data to this article can be found online at https://doi.org/10.1016/j.bios.2022.115002.

References

AbuSalah, M.A.H., Gan, S.H., Al-Hatamleh, M.A.I., Irekeola, A.A., Shueb, R.H., Yean Yean, C., 2020. Pathogens 9, 226.

Ai, J.-W., Zhou, X., Xu, T., Yang, M., Chen, Y., He, G.-Q., Pan, N., Cai, Y., Li, Y., Wang, X., Su, H., Wang, T., Zeng, W., Zhang, W.-H., 2019. Emerg. Microb. Infect. 8, 1361–1369.

An, L., Tang, W., Ranalli, T.A., Kim, H.-J., Wytiaz, J., Kong, H., 2005. J. Biol. Chem. 280, 28952–28958.
Balakrishnan, L., Bambara, R.A., 2013. Annu. Rev. Biochem. 82, 119–138.
Bronkhorst, A.J., Ungerer, V., Holdenrieder, S., 2019. Biomol. Detect. Quantif. 17, 100087.
Broughton, J.P., Deng, X., Yu, G., Fasching, C.L., Servellita, V., Singh, J., Miao, X., Streithorst, J.A., Granados, A., Sotomayor-Gonzalez, A., Zorn, K., Gopez, A., Hsu, E., Gu, W., Miller, S., Pan, C.-Y., Guevara, H., Wadford, D.A., Chen, J.S., Chiu, C.Y., 2020. Nat. Biotechnol. 38, 870–874.
Chen, J.S., Ma, E., Harrington, L.B., Da Costa, M., Tian, X., Palefsky, J.M., Doudna, J.A., 2018. Science 360, 436–439.
Cheung, S.T., Huang, D.P., Hui, A.B., Lo, K.W., Ko, C.W., Tsang, Y.S., Wong, N., Whitney, B.M., Lee, J.C., 1999. Int. J. Cancer 83, 121–126.
Collias, D., Beisel, C.L., 2021. Nat. Commun. 12, 555.
Cunningham, C.H., Hennelly, C.M., Lin, J.T., Ubalee, R., Boyce, R.M., Mulogo, E.M., Hathaway, N., Thwai, K.L., Phanzu, F., Kalonji, A., Mwandagalirwa, K., Tshefu, A., Juliano, J.J., Parr, J.B., 2021. EBioMedicine 68, 103415.
Cyranoski, D., 2021. Nature 589, 337–338.
D'Ambrosio, V., Pramanik, S., Goroncy, K., Jakočiūnas, T., Schönauer, D., Davari, M.D., Schwaneberg, U., Keasling, J.D., Jensen, M.K., 2020. Biotechnol. Notes 1, 9–15.
Daker, M., Yeo, J.T., Bakar, N., Abdul Rahman, A.S.A., Ahmad, M., Yeo, T.C., Khoo, A.S. B., 2016. Exp. Ther. Med. 11, 2117–2126.
Drain, P.K.N., 2022. Engl. J. Med. 386, 264–272.
Eis, P.S., Olson, M.C., Takova, T., Curtis, M.L., Olson, S.M., Vener, T.I., Ip, H.S., Vedvik, K.L., Bartholomay, C.T., Allawi, H.T., Ma, W.-P., Hall, J.G., Morin, M.D., Rushmore, T.H., Lyamichev, V.I., Kwiatkowski, R.W., 2001. Nat. Biotechnol. 19, 673–676.
Garforth, S.J., Ceska, T.A., Suck, D., Sayers, J.R., 1999. Proc. Natl. Acad. Sci. U. S. A. 96 (1), 38–43.
Gootenberg, J.S., Abudayyeh, O.O., Lee, J.W., Essletzbichler, P., Dy, A.J., Joung, J., Verdine, V., Donghia, N., Daringer, N.M., Freije, C.A., Myhrvold, C., Bhattacharyya, R.P., Livny, J., Regev, A., Koonin, E.V., Hung, D.T., Sabeti, P.C., Collins, J.J., Zhang, F., 2017. Science 356, 438–442.
Hartman, L.J., Selby, E.B., Whitehouse, C.A., Coyne, S.R., Jaissle, J.G., Twenhafel, N.A., Burke, R.L., Kulesh, D.A., 2009. J. Mol. Diagn. 11, 464–471.
Huang, X., Zhang, F., Zhu, K., Lin, W., Ma, W., 2021. Virus Res. 304, 198530.
Joung, J., Ladha, A., Saito, M., Kim, N.-G., Woolley, A.E., Segel, M., Barretto, R.P.J., Ranu, A., Macrae, R.K., Faure, G., Ioannidi, E.I., Krajeski, R.N., Bruneau, R., Huang, M.-L.W., Yu, X.G., Li, J.Z., Walker, B.D., Hung, D.T., Greninger, A.L., Jerome, K.R., Gootenberg, J.S., Abudayyeh, O.O., Zhang, F.N., 2020. Engl. J. Med. 383, 1492–1494.
Kaminski, M.M., Abudayyeh, O.O., Gootenberg, J.S., Zhang, F., Collins, J., 2021. J. Nat. Biomed. Eng. 5, 643–656.
Kellner, M.J., Koob, J.G., Gootenberg, J.S., Abudayyeh, O.O., Zhang, F., 2019. Nat. Protoc. 14, 2986–3012.
Kim, S., Misra, A., 2007. Annu. Rev. Biomed. Eng. 9, 289–320.
Kumar, S., Thambiraja, T.S., Karuppanan, K., Subramaniam, G.J., 2022. Med. Virol. 94, 1641–1649.
Larson, M.H., Pan, W., Kim, H.J., Mauntz, R.E., Stuart, S.M., Pimentel, M., Zhou, Y., Knudsgaard, P., Demas, V., Aravanis, A.M., Jamshidi, A., 2021. Nat. Commun. 12, 2357.
Li, S.-Y., Cheng, Q.-X., Wang, J.-M., Li, X.-Y., Zhang, Z.-L., Gao, S., Cao, R.-B., Zhao, G.-P., Wang, J., 2018. Cell Discovery 4, 20.
Li, Y., Li, S., Wang, J., Liu, G., 2019. Trends Biotechnol. 37, 730–743.
Low, J.L., Kao, P.H.-N., Tambyah, P.A., Koh, G.L.E., Ling, H., Kline, K.A., Cheow, W.S., Leong, S.S.J., 2021. Biotechnol. Notes 2, 1–10.
Lyamichev, V., Brow, M.A., Varvel, V.E., Dahlberg, J.E., 1999a. Proc. Natl. Acad. Sci. U. S.A. 96, 6143–6148.
Lyamichev, V., Mast, A.L., Hall, J.G., Prudent, J.R., Kaiser, M.W., Takova, T., Kwiatkowski, R.W., Sander, T.J., de Arruda, M., Arco, D.A., Neri, B.P., Brow, M.A.D., 1999b. Nat. Biotechnol. 17, 292–296.
Malcı, K., Walls, L.E., Rios-Solis, L., 2022. ACS Synth. Biol. 11, 1555–1567.
Munoz-Price, L.S., Poirel, L., Bonomo, R.A., Schwaber, M.J., Daikos, G.L., Cormican, M., Cornaglia, G., Garau, J., Gniadkowski, M., Hayden, M.K., Kumarasamy, K., Livermore, D.M., Maya, J.J., Nordmann, P., Patel, J.B., Paterson, D.L., Pitout, J., Villegas, M.V., Wang, H., Woodford, N., Quinn, J.P., 2013. Lancet Infect. Dis. 13, 785–796.
Navon-Venezia, S., Kondratyeva, K., Carattoli, A., 2017. FEMS (Fed. Eur. Microbiol. Soc.) Microbiol. Rev. 41 (3), 252–275.
Nguyen, L.T., Smith, B.M., Jain, P.K., 2020. Nat. Commun. 11, 4906.
Ong, J.L., Loakes, D., Jaroslawski, S., Too, K., Holliger, P., 2006. J. Mol. Biol. 361, 537–550.
Ooi, K.H., Liu, M.M., Tay, J.W.D., Teo, S.Y., Kaewsapsak, P., Jin, S., Lee, C.K., Hou, J., Maurer-Stroh, S., Lin, W., Yan, B., Yan, G., Gao, Y.-G., Tan, M.H., 2021. Nat. Commun. 12, 1739.
Qiu, M., Zhou, X.M., Liu, L.J., 2022. Anal. Test 6, 44–52.
Shen, J., Zhou, X., Shan, Y., Yue, H., Huang, R., Hu, J., Xing, D., 2020. Nat. Commun. 11, 267.
Song, Y., Gao, K., Cai, X., Cheng, W., Ding, S., Zhang, D., Deng, S., 2022. ACS Synth. Biol. 11, 3847–3854.
Tarantino, M.E., Bilotti, K., Huang, J., Delaney, S., 2015. J. Biol. Chem. 290, 21154–21162.
Teng, F., Guo, L., Cui, T., Wang, X.-G., Xu, K., Gao, Q., Zhou, Q., Li, W., 2019. Genome Biol. 20, 132.
Tóth, E., Varga, É., Kulcsár, P.I., Kocsis-Jutka, V., Krausz, S.L., Nyeste, A., Welker, Z., Huszár, K., Ligeti, Z., Tálas, A., Welker, E., 2020. Nucleic Acids Res. 48, 3722–3733.
Tzimagiorgis, G., Michailidou, E.Z., Kritis, A., Markopoulos, A.K., Kouidou, S., 2011. Cancer Epidemiol. 35, 580–589.
Vangah, S.J., Katalani, C., Boone, H.A., Hajizade, A., Sijercic, A., Ahmadian, G., 2020. Biol. Proced. Online 22, 22.
Woo, C.H., Jang, S., Shin, G., Jung, G.Y., Lee, J.W., 2020. Nat. Biomed. Eng. 4, 1168–1179.
Wu, Y., Liu, S.-X., Wang, F., Zeng, M.-S., 2019. Clin. Chem. 65, 591–592.
Wyres, K.L., Lam, M.M.C., Holt, K.E., 2020. Nat. Rev. Microbiol. 18, 344–359.
Xia, G., Chen, L., Sera, T., Fa, M., Schultz, P.G., Romesberg, F.E., 2002. Proc. Natl. Acad. Sci. U.S.A. 99, 6597–6602.
Xu, Y., Derbyshire, V., Ng, K., Chen Sun, X., Grindley, N.D.F., Joyce, C.M., 1997. J. Mol. Biol. 268, 284–302.
Yang, S., Rothman, R.E., 2004. Lancet Infect. Dis. 4 (6), 337–348.
Yoon, T., Shin, J., Choi, H.J., Park, K.S., 2022. Biosens. Bioelectron. 208, 114221.